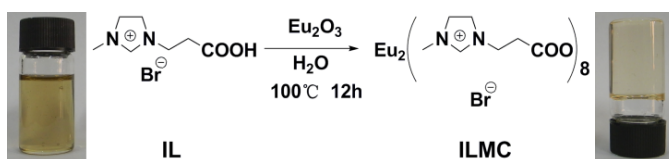


Supporting Information

A Novel Ionic Liquid-Metal Complex Electrolyte System for Remarkable Increasing in the Efficiency of Dye-sensitized Solar Cells

5 Qingqing Miao, Suojiang Zhang,* Hui Xu, Pengmei Zhang, and Huanrong Li

Synthesis of ionic liquid-metal complex (ILMC)



10

Fig. S1 The green synthetic route of ILMC.

The green synthetic route of ILMC was shown in Fig. S1.

Eu_2O_3 (4 mmol) was heated with IL (10 mmol) in 100 ml water at 100° for 12 h. The reaction mixture was filtered to remove the excess metal oxide. The obtained filtrate was processed through evaporation by rotary evaporation to remove the vast majority of water until the non-flow gel state was obtained. Subsequently, the obtained target complex was further dried in vacuum drying oven at 60° overnight. The ILMC was obtained with a transparent and light color as well as an idea gel state.^[1-2] Elemental analysis (%): calcd for $\text{Eu}_2\text{C}_{36}\text{H}_{88}\text{N}_{16}\text{O}_{20}\text{Br}_8$: Eu 13.53, C 29.90, H 3.92, N 9.97, Br 28.44; found: Eu 13.49, C 29.68, H 3.90, N 9.80, Br 28.48.

It's worth noting that the exact structure of ILMC was difficult to be confirmed by the crystal method. Correspondingly, we tentatively give the structure of ILMC based on the elemental analysis result and the coordination structures of the other Eu complexes.^[3]

The comparisons of FT-IR, Raman spectra, X-ray diffraction (XRD) patterns and TGA curves between IL and ILMC have been shown in Fig. S2- Fig. S5.

Preparation of TiO_2 photoanode

A $10\ \mu\text{m}$ thick layer of 20 nm TiO_2 (P25, Degussa, Germany) was attached to a FTO glass by screen printing technique. The obtained film was sintered at 500°C for 30 min. A scattering layer (ST41, about $5\ \mu\text{m}$) was applied with the similar procedure. After cooling to 80°C , the TiO_2 films were immersed in 5×10^{-4} M solution of N719 dye (Solaronix SA, Switzerland) in ethanol for 20 h.

Preparation of electrolytes

IL electrolyte: The IL electrolyte was prepared by adding 0.1 M I_2 , 0.1 M LiI, 1-methyl-3-propyl imidazolium iodide (PMII) into IL with the volume ratio of 3:1.

ILMC electrolyte: The ILMC electrolyte was obtained by adding 0.1 M I_2 , 0.1 M LiI and PMII into ILMC with the volume ratio of 3:1.

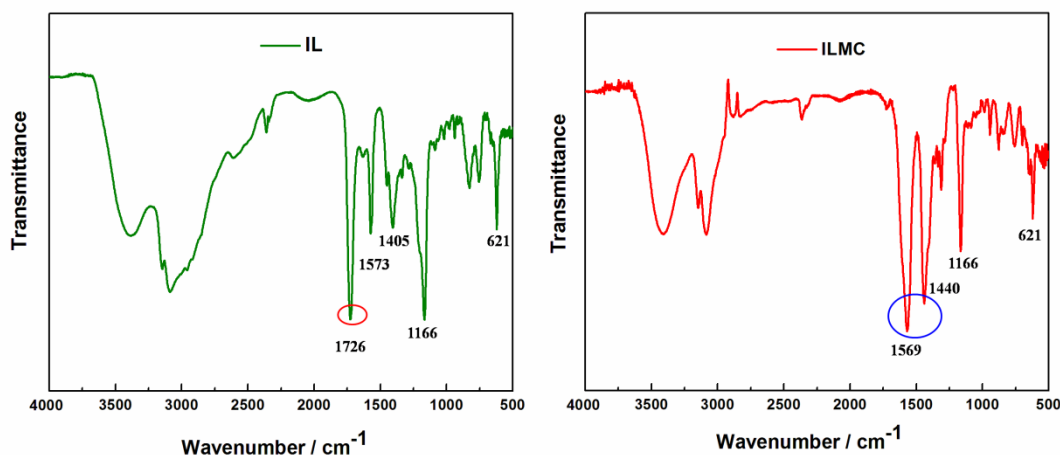
Fabrication of Solar Cells

30

The dye-sensitized photoanode (area: 0.16 cm^2) was assembled with a platinized counter electrode with the IL or ILMC electrolyte injected into the cell.

Characterization

Infrared absorption spectra were recorded on a Fourier transform infrared (FT-IR) spectrometer (Nicolet 380, USA). 5 Laser Raman spectra were studied on a laser Raman spectrometer (LabRam HR800, Horiba Jobin Yvon, France). X-ray diffraction (XRD) patterns were measured on a Bruker D8-Advance X-ray powder diffractometer with $\text{Cu K}\alpha$ radiation ($\lambda = 1.5418 \text{ \AA}$) at scanning angles 2θ from 10° to 90° . Thermogravimetric studies were analyzed by using a DSC-60A (Shimadzu, Japan) at a heating rate of $5^\circ \text{C min}^{-1}$ in a temperature range of 0°C - 600°C using dried nitrogen as purging gas. SEM images were taken by a field-emission scanning electron microscope (JSM 6700F, Japan). Current-voltage curves were conducted by a Keithley digital source meter (Keithley 2400, USA) under a solar simulator simulating the AM 1.5 spectrum (100 mW/cm^2 , Class AAA, Oriel, USA). The incident light intensity was calibrated with a standard silicon solar cell (Newport, USA). The electrochemical impedance spectroscopy (EIS, Zenium Zahner, Germany) was actualized in the dark conditions with a bias voltage corresponding to V_{OC} . The measured frequency ranged from 100 mHz to 1MHz and the AC amplitude was set at 10 mV. The ionic conductivity measurements were determined by an AC impedance technique using Zahner Zennium (Germany) with the sandwiched conductors between two identical Pt electrodes. The frequency ranged from 1Hz to 1MHz and the AC amplitude was set at 10 mV. The diffusion coefficient value (D) of I_3^- was obtained from the polarization measurements (CHI 660) with symmetrical Pt cells injected with electrolyte and sealed with surlyn film. The diffusion-limiting current density was measured by cyclic voltammetry using a scan rate of 2 mV/s .

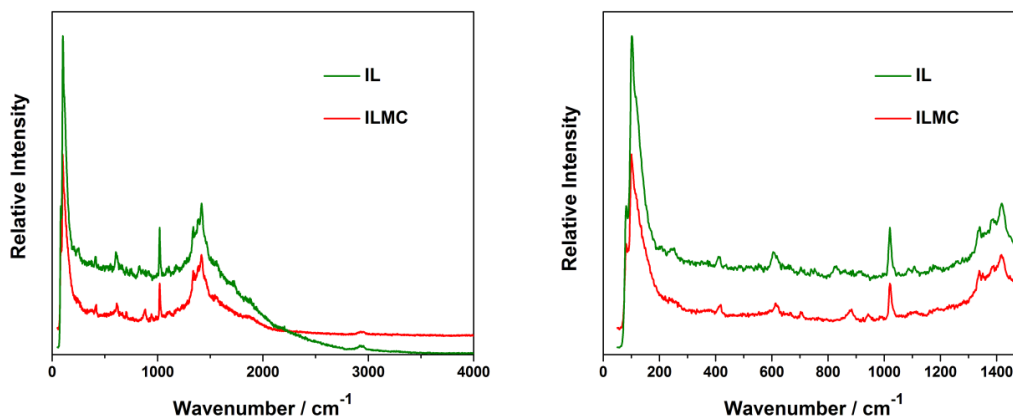


20

Fig. S2. The FT-IR spectra of IL and ILMC.

Fig. S2 shows the FT-IR spectra of IL and ILMC. The characteristic peak at 1726 cm^{-1} of IL is assigned to stretching vibration of C=O in carboxyl group. However, the characteristic peak disappeared in the spectrum of ILMC. Correspondingly, the peaks at 1573 cm^{-1} and 1405 cm^{-1} shifted to 1569 cm^{-1} and 1440 cm^{-1} , which indicate the asymmetric and symmetric stretch of the carboxylate group respectively. The result means that the carboxyl group of IL reacts with the metal oxide to form the chelate metal complex. In this reaction, water is also produced by the chelate of $-\text{COOH}$ group of IL with metal oxide. In other words, in the chelate metal complex, it is the $-\text{COO}^-$ group that coordinated with the metal

center. This can be further supported by the other similar reactions caused by the compounds with $-\text{COOH}$ group and metal oxides to form the $-\text{COO}^-$ chelated metal complexes. [2-5]



5

Fig. S3 Comparison of the Raman spectra of IL and ILMC.

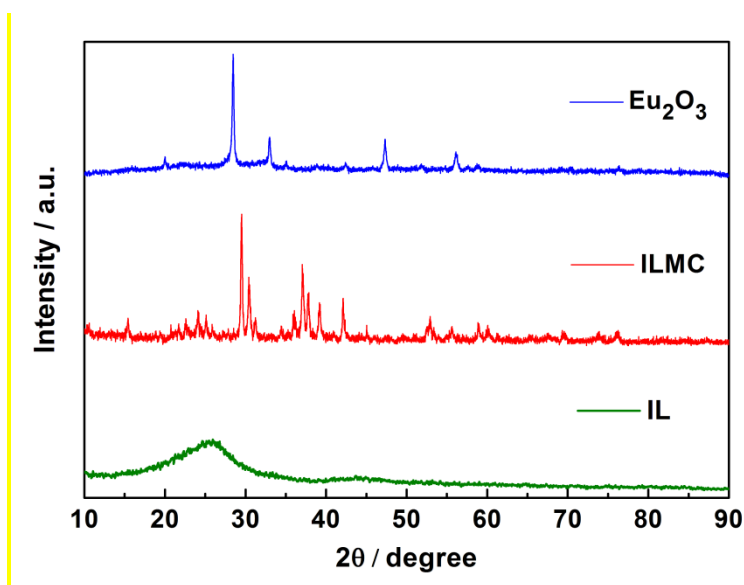


Fig. S4 Comparison of the XRD patterns of IL, Eu_2O_3 and ILMC.

As shown in Fig. S4, the synthesized ILMC has the distinct XRD pattern compared with that of IL and Eu_2O_3 , indicating that the chelate metal complex was obtained in the reaction between IL and the metal oxide. The strong and sharp diffraction peaks appearing in the XRD pattern of ILMC have obvious relevance with the well-crystallized nature of the chelate metal complex. For comparison, the XRD of Eu_2O_3 was also shown in the figure, which is accord with the standard one (PDF#65-3182).

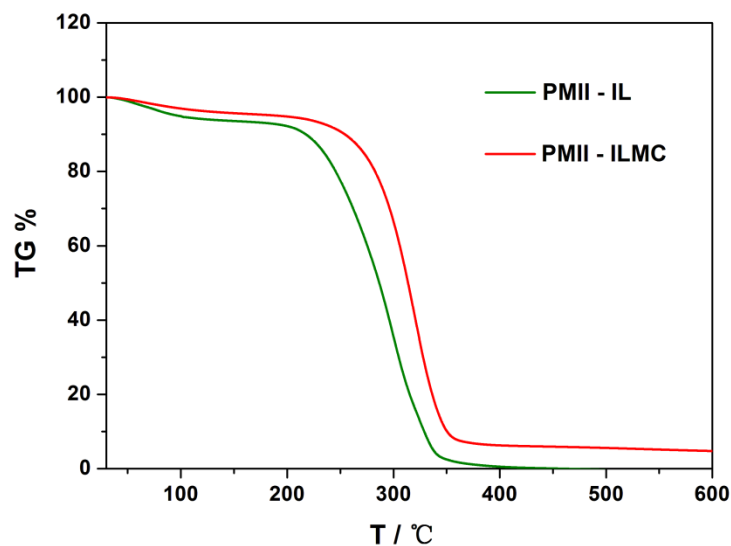


Fig. S5 The TGA curves of the IL mixtures in the IL and ILMC electrolytes.

TGA curves shown in Fig. S5 exhibit the better thermal stability of ILMC-PMII compared with IL-PMII.

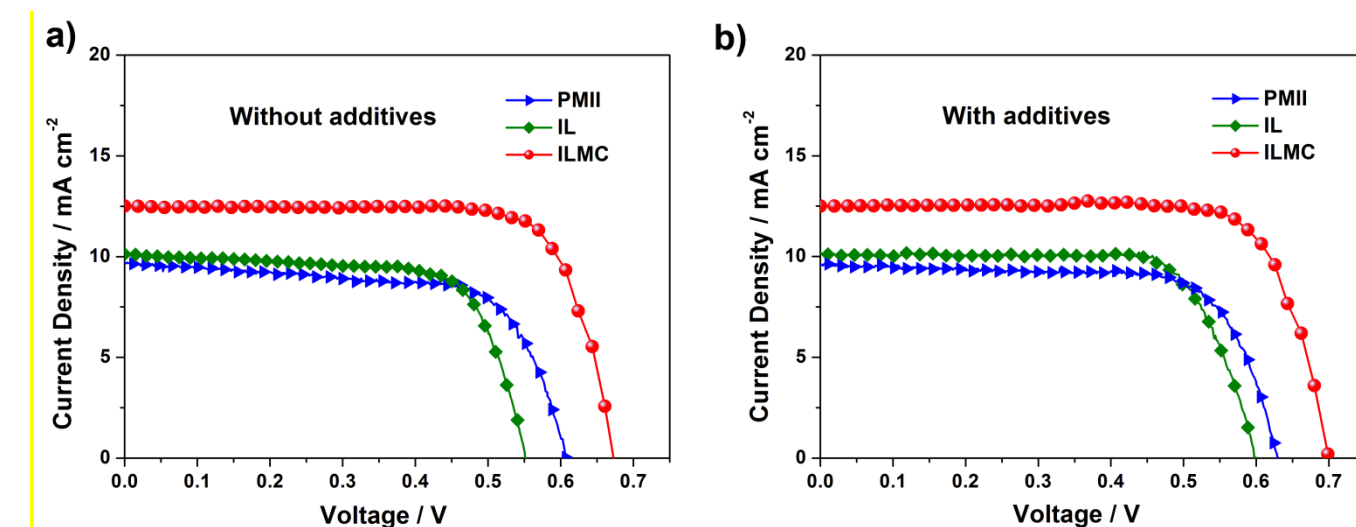


Fig. S6 The I-V curves of the PMII, IL, ILMC-based devices: a) without additives; b) with additives.

The I-V curves of the PMII, IL, ILMC-based devices were shown in Fig.S6 with the corresponding photovoltaic parameters in Table S1. The results showed that the IL with carboxyl group exhibited the similar conversion efficiency (about 4%) to the PMII in the same test conditions (without additives), which has the lowest viscosity amongst the iodide salts that form room-temperature ILs^[6], while the ILMC-based device achieved the greatly enhanced conversion efficiency of 6.49%. When the additives of TBP and GuNCS were added, all the three electrolytes obtained the enhanced efficiencies with the improved V_{oc} and slightly lower J_{sc} , which were 4.36%, 4.59%, 6.76% for PMII, IL, ILMC, respectively. These results give the further support for the superior performance of the developed novel ILMC electrolyte for DSCs.

Table S1 The photovoltaic performance of the PMII, IL, ILMC-based devices

Samples ^a	V_{oc}/V	$J_{sc}/mAcm^{-2}$	FF	$\eta/\%$
PMII-without additives ^b	0.61	9.69	0.68	4.00
IL-without additives ^b	0.55	10.13	0.71	3.99
ILMC-without additives ^b	0.68	12.51	0.76	6.49
PMII-with additives ^c	0.63	9.58	0.72	4.36
IL-with additives ^c	0.60	10.12	0.75	4.59
ILMC-with additives ^c	0.72	12.50	0.75	6.76

^a The photovoltaic performance of the DSCs were measured with the photoanodes without scattering layer under one sun illumination (AM1.5G, 100 mW cm⁻²).

^b Electrolyte composition: 0.1 M I₂, 0.1 M LiI in corresponding IL solvents.

^c Electrolyte composition: 0.1 M I₂, 0.1 M LiI, 0.5 M TBP, 0.1 M GuNCS in corresponding IL solvents.

5

References

- [1] P. Nockemann, B. Thijs, T. N. Parac-Vogt, K. V. Hecke, L. V. Meervelt, B. Tinant, I. Hartenbach, T. Schleid, V. T. Ngan, M. T. Nguyen and K. Binnemans, *Inorg. Chem.* **2008**, 47, 9987-9999.
- 10 [2] H. Li, P. Liu, H. Shao, Y. Wang, Y. Zheng, Z. Sun and Y. Chen, *J. Mater. Chem.* **2009**, 19, 5533-5540.
- [3] P. Nockemann, B. Thijs, K. Lunstroot, T.N. Parac-Vogt, C. Göller-Walrand, K. Binnemans, K. V. Hecke, L. V. Meervelt, S. Nikitenko, J. Daniels, C. Hennig and R.V. Deun, *Chem. Eur. J.* **2009**, 15, 1449-1461.
- [4] L. Lu, F. Liu, G. Sun, H. Zhang, * S.Xi and H. Wang, *J. Mater. Chem.*, **2004**, 14, 2760 – 2762.
- [5] P. Nockemann,* B. Thijs, K. V. Hecke, L. V. Meervelt and K. Binnemans, *Crystal Growth & Design*, **2008**, 8, 1353–1363.
- 15 [6] Y. Bai, Y. Cao, J. Zhang, M. Wang, R. Li, P. Wang, S. M. Zakeeruddin and M. Grätzel, *Nat. Mater.*, **2008**, 7, 626.

